

Deep Learning System Boundary Testing through Latent Space Style Mixing

Amr Abdellatif

Technical University of Munich
Munich, Germany
amr.abdellatif@tum.de

Vincenzo Riccio

Università degli Studi di Udine
Udine, Italy
vincenzo.riccio@uniud.it

Xingcheng Chen

Technical University of Munich, fortiss GmbH
Munich, Germany
xingcheng.chen@tum.de, xchen@fortiss.org

Andrea Stocco

Technical University of Munich, fortiss GmbH
Munich, Germany
andrea.stocco@tum.de, stocco@fortiss.org

Abstract—Evaluating the behavioral frontier of deep learning (DL) systems is crucial for understanding their generalizability and robustness. However, boundary testing is challenging due to their high-dimensional input space. Generative artificial intelligence offers a promising solution by modeling data distribution within compact latent space representations, thereby facilitating finer-grained explorations.

In this work, we introduce MIMICRY, a novel black-box system-agnostic test generator that leverages these latent representations to generate frontier inputs for the DL systems under test. Specifically, MIMICRY uses style-based generative adversarial networks trained to learn the representation of inputs with disentangled features. This representation enables embedding style-mixing operations between a source and a target input, combining their features to explore the boundary between them. We evaluated the effectiveness of different configurations of MIMICRY at generating boundary inputs for four popular DL image classification systems. Our results show that manipulating the latent space allows for effective and efficient exploration of behavioral frontiers. As opposed to a model-based baseline, MIMICRY generates a higher quality frontier of behaviors which includes more and closer inputs. Additionally, we assessed the validity of these inputs, revealing a high validity rate according to human assessors.

I. INTRODUCTION

The increasing dependence on Deep Learning (DL) systems for both everyday tasks and critical sectors [1] makes rigorous testing for these systems a relevant topic [2], [3]. The concept of fault in DL systems is more complex than in traditional software [2]. Even if the code that builds the DL network is bug-free, the trained DL model may still deviate from the expected behavior due to faults introduced during the training phase, such as the misconfiguration of learning parameters or the use of an unbalanced or non-representative training set [4]. In the context of data-intensive software systems, such as DL systems, faults often arise from the large, high-dimensional input space, which requires the generation of test data that accurately captures the complexity and diversity of the validity domain, i.e., the portion of the input space for which the system is designed to operate correctly [2].

Test generation techniques have been developed to produce artificial inputs that induce unexpected behaviors in DL systems [2], [3], [5]–[9]. The main goal of these techniques is to achieve high failure exposure and/or high values of DL-specific adequacy metrics, such as neuron [10] or surprise coverage [11]. However, these techniques often neglect a thorough exploration of the input space of DL systems, especially in regions that are critical for decision making.

In particular, boundary testing focuses on those regions of the input space where slight changes can trigger different behaviors of the DL system. These inputs are extremely relevant for assessing the reliability of DL systems, as they often reveal how the system handles edge cases and transitions between different operational domains. However, boundary testing for DL systems is challenging due to the lack of precise input partitions and the unconstrained nature of the inputs that they are expected to handle (e.g., images).

Few techniques in the literature address DL boundary testing [12]. One notable example is DeepJanus [5], a model-based input generation technique that uses the concept of the frontier of behaviors. This frontier refers to a collection of input pairs that exhibit similarity within the pair, yet trigger different behaviors. While DeepJanus represents a competitive approach, it assumes the availability of a high-fidelity model representation of the input domain which can be manipulated to generate test inputs. However, for most DL benchmarks such as complex feature-rich image datasets, a model representation is not available, limiting the application of boundary testing. Recent advances in generative artificial intelligence promise to overcome this limitation, as they can learn a lower-dimensional representation of the input space (i.e., the *latent space*) based on the observed data distribution, facilitating input manipulation. Although there are existing methods to generate inputs in the latent space of a DL model [13]–[16], none of them focuses on generating boundary inputs.

In this paper, we propose a technique to effectively explore the boundary of DL systems in the latent space of style-based generative adversarial networks. The key idea behind using

these networks involves leveraging their style transfer architecture that automatically learns the separation of high-level attributes (e.g., shape) from lower-level ones (e.g., texture). While primarily used for the generation of new, highly diverse datasets of complex inputs, in this work, we leverage the scale-specific control of the synthesis and disentangle latent factors of variation for boundary testing of DL systems.

Our technique, implemented in a tool called MIMICRY, uses style-mixing operations to find boundary inputs. To do so, MIMICRY uses a StyleGAN model trained to learn the visual characteristics of a given image dataset across all its inputs. StyleGAN maps latent vectors inputs to an intermediate latent vector, called *style vector*, which controls the image style at various granularity levels in the generative process. The main idea of MIMICRY involves the systematical mutation of the pre-defined set of style vectors between source and target inputs using scale-specific style mixing and assessing the impact of these modifications in the image space.

MIMICRY provides *focused* generation of boundary inputs. For a given source input, MIMICRY identifies the boundary exploration *direction* based on the confidence level of the DL system, specifically targeting the second most probable class for that input, by generating a target input for that class. Subsequently, it alters the visual characteristics of the source input using the latent code from the target input.

We have evaluated the effectiveness of MIMICRY on four popular image classification datasets (MNIST, SVHN, FashionMNIST, CIFAR-10) using DL systems available from the literature. Our experiments, comprising over 1,600 test cases, show that MIMICRY identifies a significant number of frontier inputs for both closer or farther to the boundary seeds. Additionally, our study shows that the boundary inputs generated by MIMICRY are valid, exhibiting a high validity rate (81%) and label preservation rate (65%) as evaluated by human assessors. Finally, MIMICRY outperforms the model-based DeepJanus approach in both effectiveness and label coverage. Our paper makes the following contributions:

Technique. To the best of our knowledge, the first boundary testing technique for DL systems based on style-mixing.

Evaluation. An empirical study shows that MIMICRY is more effective than an existing model-based technique, including higher validity and label-preservation rates.

II. BACKGROUND

A. Boundary Analysis of DL Systems

Boundary analysis can identify minimal changes in test inputs that lead to notably different behaviors of the DL system under test. Several testing approaches emphasize boundary analysis [17] due to its effectiveness in debugging by isolating input features that are responsible for different system behaviors, e.g., a correct prediction and a misprediction in an image classification task. These test generators aim to produce pairs of inputs where the members of the pair are similar among them but produce different behaviors [5]. Many of these approaches use search-based or optimization techniques

to identify boundary inputs, although their generalizability to complex data-intensive systems such as DL might require specific adaptations [5], [18]–[20]. The main goal of these approaches is to ensure similarity within the input pair and the validity of the generated inputs. In this work, we aim to explore these boundaries using advanced generative artificial intelligence algorithms that allow a controllable search, targeted at specific boundary regions by manipulating inputs at predefined granularities.

B. Style-Based Generative Adversarial Networks

Generative Adversarial Networks (GANs) are algorithms designed to learn the statistical distribution of the underlying training dataset, allowing the synthesis of new samples that are representative of the learned distribution [21], [22]. GANs involve jointly training a pair of networks that compete with each other. This approach is based on game theory and is implemented by using two neural networks. A first neural network, called the generator, aims to produce realistic images, while a second neural network, called the discriminator, acts as an expert that receives both fake and real (authentic) images and aims to distinguish between them. In this way, the generator improves its ability to produce realistic images by learning to fool the discriminator, which can be leveraged for test generation [13], [14], [16], [23].

StyleGAN [24] extends the GAN architecture to introduce new methods for controlling the image synthesis process. Unlike traditional GANs, StyleGAN enables style control at multiple levels within the network. The proposed changes to the generator model involve the use of a mapping network to map points in the initial latent space to an intermediate latent space. This intermediate latent space controls the strength of image features at various scales in the generator model, inspired by style transfer literature [25]. This architectural change, combined with noise injected directly into the network, enables the automatic, unsupervised separation of high-level attributes from stochastic variations in the generated images. For test generation, StyleGANs provide precise control over input synthesis and manipulation, which we exploit for boundary testing.

III. APPROACH

MIMICRY is a black-box approach¹ that leverages StyleGANs to generate boundary inputs through *targeted* search. It begins by generating a source latent vector (called *source seed*) which belongs to a user-specified class, i.e., the source class. Based on the confidence of the DL system under test for the source seed, MIMICRY selects a target class. Then, it generates a *target seed* belonging to the target class, and applies focused style-mixing mutations to identify the boundary between the source and target seeds by combining their features.

¹A recent survey classifies methods that need access to both the training and test datasets of a learned component as *data-box* methods. However, to avoid confusion, we refer to these as black-box methods, since they do not utilize any internal information from the model itself. [2].

Algorithm 1: MIMICRY

Input : \mathcal{D} : deep learning system under test
 $class_{source}$: class of the source seed
 S_{max} : max number of style-mix operations
 \mathcal{L} : list of the style layer combinations
 \mathcal{F}_{size} : failure set size
Output: \mathcal{F} : archive of best boundary inputs

```

1  $\mathcal{F} \leftarrow \emptyset$ 
2 while  $|\mathcal{F}| < \mathcal{F}_{size}$  do
3    $source \leftarrow \text{GENERATESEED}(class_{source})$ 
4    $image \mathcal{I} \leftarrow \text{GENERATEIMAGE}(source)$ 
5    $prediction p, confidenceScores \leftarrow \text{PREDICT}(\mathcal{D}, \mathcal{I})$ 
6   if  $p = class_{source}$  then
7      $styleMixCounter \leftarrow 0$ 
8      $foundMix \leftarrow \text{false}$ 
9      $\mathcal{J} \leftarrow \emptyset$ 
10    while not foundMix and styleMixCounter < S_{max} do
11       $class_{target} \leftarrow \text{GETCLASS}(confidenceScores)$ 
12       $target \leftarrow \text{GENERATESEED}(class_{target})$ 
13      foreach  $l \in \mathcal{L}$  do
14         $mix \leftarrow \text{STYLEMIX}(source, target, l)$ 
15         $image \mathcal{M} \leftarrow \text{GENERATEIMAGE}(mix)$ 
16         $prediction p, confidenceScores \leftarrow \text{PREDICT}(\mathcal{D}, \mathcal{M})$ 
17        if  $p \neq class_{source}$  then
18           $foundMix, \mathcal{J} \leftarrow \text{EVALUATEPAIR}(\mathcal{I}, \mathcal{M}, \mathcal{J})$ 
19          if foundMix then
20            BREAK
21       $styleMixCounter \leftarrow styleMixCounter + 1$ 
22     $\mathcal{F} \leftarrow \mathcal{F} \cup (< \mathcal{I}, \mathcal{J} >)$ 
23  return  $\mathcal{F}$ 

```

Algorithm 1 shows the main steps of MIMICRY. Our approach takes as input the DL system, the source class $class_{source}$, the maximum number of style-mixing mutation operations S_{max} , and the list of layer combinations used for style mixing \mathcal{L} . The termination condition is met when the testing budget is exhausted, e.g., by finding the desired number of solutions in the failure set (\mathcal{F}_{size}).

Initially, the failure set \mathcal{F} is empty (Line 1). Then, the main loop of the algorithm (Lines 3–22) generates source seeds and applies focused style-mixing mutations on them until either a failure is found or the budget of style-mixing mutations S_{max} is exhausted. Specifically, at every iteration, a latent vector of class $class_{source}$ is generated by StyleGAN (Line 3) and decoded to the pixel space into an actual image \mathcal{I} (Line 4). Then, the input image is evaluated by the DL system \mathcal{D} (Line 5). If the input results in a *failure* (i.e., the predicted class is different from the source class), then no further test generation is necessary: the input is already beyond the boundary and it is discarded. Otherwise, the main style-mixing cycle starts (Lines 10–21). Based on the DL system’s per-class confidence scores, MIMICRY determines the boundary exploration direction (Line 11) leveraging the DL system’s uncertainty between two classes.

Then, a *target* seed is generated for the $class_{target}$ (Line 12) and style-mixed with the *source* seed, using different layers combinations (Line 13). Once a new style-mixed input is generated, it is decoded to the pixel space into an actual image \mathcal{M} (Lines 15–16) and evaluated by the DL system (Line 16). In case of failure, the distance between the boundary input pairs is evaluated (Line 18). If the distance constraint is satisfied, the algorithm stores the found boundary input pairs $\mathcal{J} = \mathcal{M}$

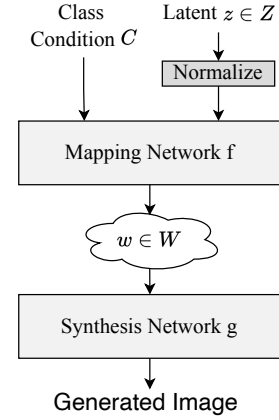


Fig. 1. Architecture of StyleGAN [24].

into the failure set (Line 22). Otherwise, it stores the best-found solution to \mathcal{J} and continues the search until the iteration budget S_{max} is exhausted (Line 21); finally, the algorithm returns the failure set \mathcal{F} (Line 23).

A. StyleGAN

Our approach uses a conditional StyleGAN [24], which allows for style control of the generated images. The StyleGAN generator has two main components: the Mapping Network and the Synthesis Network (see Figure 1). The generator uses the mapping network to map points in the latent space to an *intermediate latent space*. This intermediate latent space controls the style of image feature strength at different scales in the generator model. This architecture, combined with injected noise, enables the automatic, unsupervised separation of high-level attributes from stochastic variations in the generated images, as well as scale-specific mixing operations.

1) *Mapping Network*: The mapping network, denoted as $f : [Z, C] \rightarrow W$, is composed of eight fully connected layers that transform the initial latent input vector $z \in \mathbb{R}^{512}$ that is conditioned with a one-hot encoding class vector $c \in C$ into an intermediate latent output vector $w \in \mathbb{R}^{512}$. The reason for this conversion is that the manipulation of latent vectors in the latent space Z may yield non-linear changes in the image, as observed by previous studies [13], [14], [16], [26]. For example, absent features in either endpoint may appear in the middle of a linear interpolation path. This indicates that the latent space is entangled and the factors of variation are not properly separated. The addition of a mapping network before the generator enhances the separability in the intermediate latent space W , since the synthesis network prioritizes a disentangled input representation [24].

2) *Synthesis Network*: The Synthesis Network generates the final output images \mathcal{I} given intermediate latent vector w of an input of class $class_{source}$ (GENERATESEED procedure in Algorithm 1). It is composed of layers that control coarse, middle, and fine features. Specifically, each layer takes the intermediate latent vector w and transforms it into different levels of the *style vectors*. The generated input is then fed

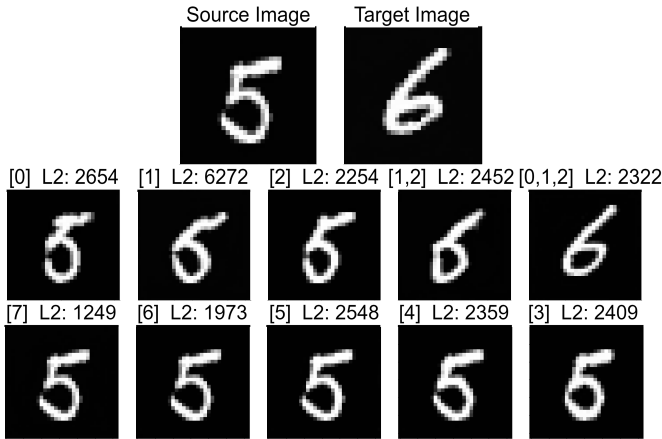


Fig. 2. Style-Mix Mutation Operator between a source seed of class “5” and a target seed of class “6” for MNIST (top). Titled with [x]: Selected Layer combination, L2: Euclidean distance between original and mutated image.

to the DL system under test, and the prediction and the confidence scores for each class are retrieved (GETCLASS procedure in Algorithm 1). In particular, we measure the confidence using the output of the softmax layer of the image classifiers under test, as is extensively done in the literature [5], [8], [13], [27], [28]. If the prediction does not match the $class_{source}$, a failure is found. Otherwise, the source seed input is considered further and MIMICRY determines the boundary exploration target class based on the DL system’s softmax output. For instance, when the softmax output shows a non-zero confidence value for a class different from class $class_{source}$, MIMICRY will use this information to narrow down the search space and designate such class as the target class ($class_{source}$ in Algorithm 1) in the boundary exploration process.

B. Style-Mix Mutation Operator

The mutation operation in MIMICRY performs “style mixing” that can be regarded as a latent-aware semantic (style and architecture) mutation operator (STYLEMIX procedure in Algorithm 1). This method involves swapping specific *style vectors* between the source and target seeds. The style vectors are latent vectors of the intermediate latent representation corresponding to specific layers of the generator. Specifically, this operation modifies the intermediate latent representation of the source input seed by replacing one of its style vectors with a style vector from the target seed. The modified intermediate latent representation is then used to generate a new input that incorporates visual features from the target input seed. This process enables the synthesis network to create variations that blend characteristics of both the source and target inputs, enabling the exploration of the boundary.

The layers in the synthesis network utilize the *style vectors* of three types [24]: coarse (layers 0-2), middle (layers 3-6), and fine (layer 7). The primary challenge is selecting which styles to swap, given there are $2^8 = 256$ possible combinations

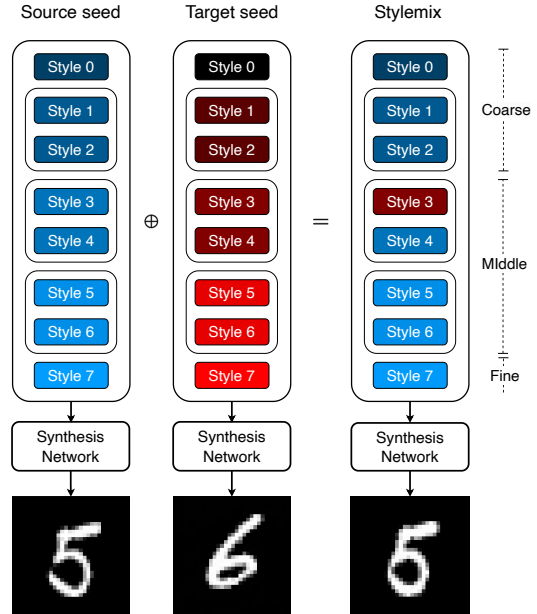


Fig. 3. An example of the StyleMix mutation operator.

of vectors. Our selection of styles takes into account two objectives: first, to minimize the extent of variation and preserve the original label, and second, to prevent hallucinations that may happen due to entangled layers within or between style blocks. Following the guidelines of the original StyleGAN paper [29], replacements in the coarse styles (in layers 0-2), which underpin the fundamental characteristics of an image, are avoided (as shown in the second row of Figure 2). This decision restricts selections to styles 3 through 7, which have moderate to fine influence on the image’s details (as shown in the third row of Figure 2). To prevent hallucinations that may arise in rare cases from layer entanglement, both layers in the same style block [3, 4], [5, 6] are also retained. Ultimately, our approach results in a total of eight possible layer combinations: [7], [6], [5], [4], [3], [5, 6], [3, 4], and [3, 4, 5, 6].

Example. Figure 2 shows an example of handwritten MNIST digits generated by MIMICRY using different layers. Consider a source input seed of $class_{source} = 5$ for which the model produces the following softmax vector: [0.05, 0.05, 0.05, 0.05, 0.05, 0.4, 0.2, 0.05, 0.1, 0.1]. The likelihood for class 5 is 0.4 (highest), while the likelihood for class 6 is 0.2 (second highest), indicating indecision between these two classes. Thus, from the point of view of boundary testing, it makes sense to navigate the latent space towards class 6. Consequently, MIMICRY generates a target input seed of $class_{target} = 6$, which is then used for boundary exploration through style-mixing. Figure 3 shows an example of an application of the style-mix mutation operator. The intermediate latent codes of seed for the source class “5” and target class “6” are represented as a stack of style vectors (Style 0-7). MIMICRY replaces the style vector “Style 3” of the source seed with that of the target seed. It results in

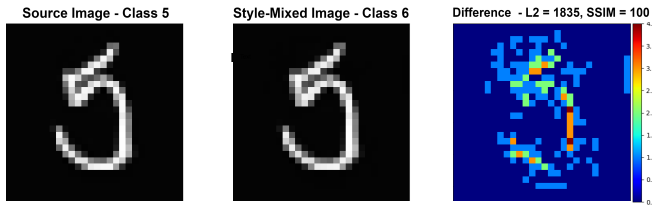


Fig. 4. Boundary pair generated by MIMICRY.

the misclassification as class “6” after imposing an amount of style-mix-induced modification. The mutation process selectively swaps specific styles following the possible layer combinations and subsequently evaluates the effect of these replacements on inducing a class change. Figure 2 shows some possible style-mix mutations given a source and a target seeds and highlights how the coarse style vectors produce more noticeable modifications.

C. Distance Function

To control the extent of the modifications induced by style mixing, we use a distance function that takes into account modifications both at the feature level and the pixel level. To assess the preservation of the characteristics of the original image after modifications, we employ the Structural Similarity Index [30] (SSIM). This metric evaluates the similarity between the original and modified images across three dimensions: luminance, contrast, and structure. On the other hand, to account for pixel-level differences between the original image and its modified version, we adopt the Euclidean norm, or l_2 norm. Particularly, we define the distance metric for MIMICRY by combining these two measures as follows:

$$SSIM(o, m) > \epsilon_{SSIM} \wedge (1 + \epsilon_{l_2}) \times l_2(o) > l_2(o - m) > 0$$

where o is the original image, m is the modified input, ϵ_{SSIM} is the structural similarity index threshold, and ϵ_{l_2} is the Euclidean norm threshold. Our goal is twofold: (1) ensuring high structural similarity and (2) minimizing the relative change with the source input seed o . The former is controlled by the ϵ_{SSIM} threshold. As for the latter, we consider the norm of the original image $l_2(o)$ and determine that, for each mutated input o , $l_2(m)$ should be less than $l_2(o) * (1 + \epsilon)$, where ϵ determines the acceptable level of alteration.

Our distance function is designed to ensure that the modified image m is both perceptually similar to the original image o but sufficiently different in terms of l_2 norm. MIMICRY uses it as an early stopping criteria (*foundMix* in Algorithm 1) to effectively navigate the latent space, leveraging the strengths of each metric to minimize variation effectively and preserve the original characteristics of the image (EVALUATEPAIR procedure in Algorithm 1).

An example of boundary input that retains high perceptual and quantitative similarities is illustrated in Figure 4.

IV. EMPIRICAL STUDY

A. Research Questions

We consider the following research questions:

RQ₁ (Effectiveness): How effective is MIMICRY at finding boundary inputs?

RQ₂ (Output Validity): To what extent are the inputs generated by MIMICRY valid, label- and target-preserving?

RQ₃ (Performance): How efficient is MIMICRY at finding boundary inputs?

RQ₄ (Configuration): Which layers utilized by MIMICRY for style mixing most frequently produce misbehaviors?

RQ₅ (Comparison): How does MIMICRY compare with an existing model-based baseline?

RQ₁ assesses whether MIMICRY generates a large number of boundary inputs. RQ₂ studies the quality of the inputs produced by MIMICRY, assessed by human evaluators. RQ₃ evaluates which layers of MIMICRY yield the best results. RQ₄ evaluates the efficiency. Finally, the last research question (RQ₅) compares MIMICRY with DeepJanus, a state-of-the-art boundary input generator for DL systems.

B. Objects of Study

In our study, we used four image classification datasets, namely MNIST [31], FashionMNIST [32], SVHN [33], and CIFAR-10 [34]. MNIST, FashionMNIST and SVHN are selected as they are used in the experimental studies of the baselines of our work, DeepJanus [5], [26], which requires a model of the input. CIFAR-10 is used to demonstrate the generalizability of our approach to datasets where a model input representation is not available.

MNIST. Handwritten digits dataset [31] consisting of 28×28 greyscale images labeled with the corresponding digit (the possible classes range from 0 to 9). MNIST has 60,000 training inputs and 10,000 test inputs. In this paper, we test a convolutional deep neural network architecture provided in the replication package of DeepJanus [5]. This model has 1.2M parameters and achieves 99.11% accuracy on the test set.

FashionMNIST. Another dataset consisting of 28×28 greyscale images of Zalando’s articles belonging to 10 categories [32]. The dataset has more complex patterns and variations than MNIST and contains 60,000 images for training and 10,000 for testing. We used a pre-trained DL model available in the literature [14], which has 1.6M parameters and achieves 93.58% accuracy on the test set.

SVHN. A more complex dataset contains 32×32 color digits of house numbers cropped from Google Street View images [33]. It has 73,257 training inputs and 26,032 test inputs. The classification task is particularly challenging due to variations in lighting, background clutter, and the presence of distracting digits adjacent to the digit of interest. To make it compatible with our baseline DeepJanus, we converted the digits to grey-scale images in the study of this paper. As for the system under test, we trained the ALL-CNN [35] model from the literature [14]. The model has 1.2M parameters and 7 convolutional layers without any dense layers, and obtained a 95.63% accuracy on the test set.

CIFAR-10. Another standard benchmark for image classification tasks is divided into 10 classes of different objects [34] and split into 50,000 training images and 10,000 testing images. Although the images are small (32×32 pixels), they contain visual complexities and variations of real-world objects, which increases the difficulty of requiring models to extract meaningful features from low-resolution images. We adopt Vision Transformer [36] with $86M$ parameters as the DL model under test and retrain it with the CIFAR-10 dataset, achieving a 97.47% accuracy on the test set.

C. Baseline

To assess the relevance of our approach, in RQ₄ we compare MIMICRY against DeepJanus, a state-of-the-art test generator for the exploration of the frontier of behaviors of DL systems. DeepJanus uses a multi-objective search-based algorithm to mutate the control points of a model of the inputs, to generate pairs of inputs that are close to each other, yet produce different behaviors of the DL system [5]. The input model representation is obtained through a vectorization operation, which produces a sequence of control points that can be adjusted to achieve slight modifications. The input image can then be reconstructed through a rasterization operation. Our comparison focused on the MNIST, FashionMNIST, and SVHN datasets, as DeepJanus’s model representation supports these benchmarks. For CIFAR-10, DeepJanus is not applicable since an appropriate input model is not available for such a feature-rich dataset, and cannot be created with the adopted vectorization-rasterization approach, as noted by its authors [5], [26].

D. Configurations

For MNIST, FashionMNIST, and SVHN, we trained a StyleGAN network, following the training configurations and guidelines of the original paper [37]. To monitor the model’s performance during training, we used the Fréchet Inception Distance (FID) metric [38]. The final FID score obtained is 0.91 for MNIST, 2.34 for FashionMNIST and 4.2 for SVHN, which is in line the original paper [37]. For CIFAR-10, we used pre-trained StyleGAN networks available in the literature [29]. Concerning our distance function and its thresholds, we used $\epsilon_{SSIM} > 95\%$ and $\epsilon_{l_2} = 0.2$. These values were selected based on a trial run on 100 seeds to find best-found frontier pairs under 1,000 StyleMix operations.

E. Procedure

Our approach requires generating seeds using StyleGAN by sampling latent vectors, which must be inspected for validity before use. For each dataset, we generated 2,000 seeds, uniformly distributed across classes, ensuring they were correctly classified by the DL models under test. Then, two authors performed a screening task by independently manually assessing the validity and label preservation of the seeds. Each author verified the class of each generated seed (e.g., which digit, piece of clothing, or object is present in each seed image). We retained only the seeds for which there was a

consensus, resulting in our final pool of seeds for the study: 200 seeds per dataset, of which 100 *partial-confidence* (C_p) seeds and 100 *full-confidence* (C_f) seeds. In the former case, the seeds are classified correctly, but with less than 100% confidence, i.e., the softmax output is less than 1.0 for the target class. In the latter case, the seeds are classified correctly with 100% confidence, i.e., the softmax output is 1.0 for the target class. The distinction between C_p and C_f allows us to evaluate MIMICRY in different scenarios. Particularly, the second configuration is used to assess MIMICRY in the worst case, where no guidance by the DL model is available and the seeds are far from the boundary.

We applied MIMICRY to all validated seeds to reduce the inherent randomness of the approach. Specifically, we ran each configuration of MIMICRY twice, using both *partial-confidence* and *full-confidence* seeds. We used a budget of 100 iterations for all datasets. This upper bound value was experimentally found adequate for convergence of MIMICRY. Concerning RQ₂, we evaluate validity and label preservation by employing human assessors. The questionnaire contains 36 generated inputs for each dataset, and 144 in total, where 90 ($36 + 18 \times 3$ from 4 datasets) misclassified inputs are produced by MIMICRY and 54 (18×3 from 3 datasets) produced by DeepJanus as the baseline. For each human assessor, a certain amount of images are randomly sampled from the generated input set to ensure equal opportunities among different configurations and inputs. We conducted a questionnaire where 17 participants were recruited from personal contacts using convenience sampling [39] and were asked to identify the class or to indicate if it was unrecognizable. This method allowed us to assess both the validity (if the response was a correct class) and label preservation (if the response matches the intended label). Concerning RQ₅, we evaluate DeepJanus on MNIST, SVHN, and FashionMNIST datasets since for CIFAR-10 a model of the input for CIFAR-10 is not available. For each dataset, we executed DeepJanus using a budget of 1,000 iterations, using the default settings of the original paper.

F. Metrics

Concerning RQ₁, we evaluate the effectiveness of the test generation technique by computing the *number of boundary inputs* found within a given number of mutation iterations across different configurations. For our DL systems, a failure corresponds to a misclassification. For RQ₂, we present the validity, label- and target-preservation rates based on the human evaluation study. For RQ₃, we assess which layers of StyleGAN most frequently trigger misbehaviors when used by MIMICRY’s mutation operator. About RQ₄, we evaluate the performance of MIMICRY by computing by the number of detected boundary inputs over the number of iterations. For the comparison with the baseline in RQ₅, we use the number of boundary inputs as in RQ₁. Moreover, we assess *label coverage*, computed as the number of target labels for which MIMICRY successfully finds boundary inputs divided by the total number of misclassified labels. This metric helps evaluate the output diversity of the boundary inputs generated by the

TABLE I
 RQ₁: EFFECTIVENESS (TOP) AND RQ₂: VALIDITY AND LABEL PRESERVATION RESULTS (BOTTOM).

	C_p : Partial Confidence				C_f : Full Confidence			
	No Target Class Preservation		Preserve Target Class		No Target Class Preservation		Preserve Target Class	
	within D_c	w/out D_c	within D_c	w/out D_c	within D_c	w/out D_c	within D_c	w/out D_c
Effectiveness								
MNIST	85	13	52	30	24	40	1	7
F-MNIST	80	19	81	18	3	74	0	17
SVHN	85	15	83	17	1	70	0	13
CIFAR-10	70	30	71	29	0	100	0	93
Output Validity								
MNIST	0.98 / 0.97	1.00 / 0.80	0.98 / 0.95	0.86 / 0.62	0.97 / 0.93	0.98 / 0.93	1.00 / 1.00	0.87 / 0.87
F-MNIST	0.97 / 0.77	0.90 / 0.57	0.91 / 0.72	0.95 / 0.68	1.00 / 1.00	0.92 / 0.66	- / -	0.90 / 0.65
SVHN	0.78 / 0.68	0.90 / 0.80	0.71 / 0.63	0.78 / 0.78	0.75 / 0.75	0.77 / 0.69	- / -	0.81 / 0.71
CIFAR-10	0.82 / 0.67	0.72 / 0.49	0.80 / 0.61	0.84 / 0.39	- / -	0.60 / 0.40	- / -	0.62 / 0.39

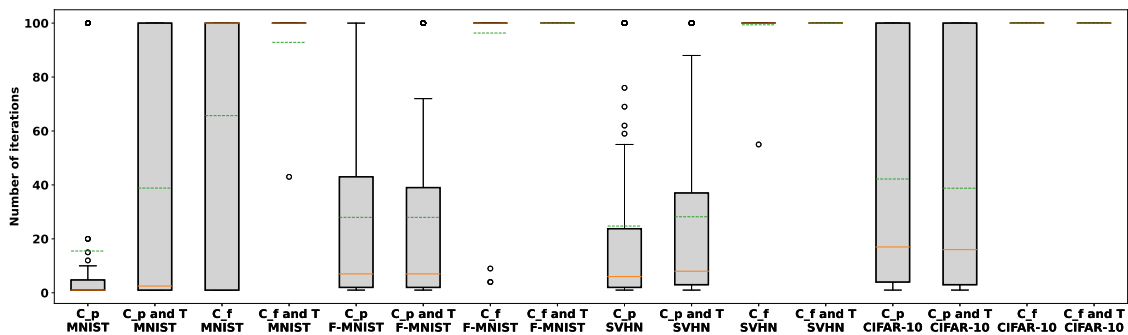


Fig. 5. RQ₃: Efficiency results.

techniques, indicating whether the boundary inputs sampled on the frontier span multiple classes or are limited to a few. Finally, we evaluate the validity and label preservation of these boundary inputs.

G. Results

1) *RQ₁ (Effectiveness)*: Table I (top) shows the average effectiveness results, for each dataset. The results are presented separately for partial-confidence seeds (C_p) and full-confidence seeds (C_f). The results are further divided into boundary inputs that achieve target preservation (i.e., the misclassification pertains to the target seed) and that respect the distance metric constraints D_c (Section III-C). Overall, MIMICRY is able to find a high number of boundary inputs across all configurations. For partial-confidence seeds and target class preservation, MIMICRY found boundary inputs for 98% of the seeds (MNIST), 99% of the seeds (FashionMNIST), and 100% of the seeds (SVHN and CIFAR-10), with the large majority being within the distance constraints D_c . Without target class preservation, the magnitude of the boundary inputs within the distance constraints D_c changes substantially only for MNIST (-38%). For full-confidence seeds, MIMICRY was successful even if it was more challenging to find boundary inputs within the given budget. This was expected, as these seeds are farther from the boundary. In

fact, most inputs are not within the distance constraints D_c , which means that image manipulations of higher magnitude are necessary to cause failures.

RQ₁: MIMICRY is able to find boundary inputs for all datasets and configurations, both for partial-confidence seeds ($\approx 97\%$) and full-confidence seeds ($\approx 55\%$).

2) *RQ₂ (Output Validity)*: Table I (bottom) presents the validity and label preservation rate for the different configurations of MIMICRY. For all datasets, the boundary inputs exhibited a high validity rate, particularly for MNIST and FashionMNIST. Although the scores for SVHN and CIFAR-10 are slightly lower, they still exceed 60%, suggesting that the inputs from these datasets are more challenging. A significant portion of the boundary inputs are also label-preserving, which highlights the high quality of the boundary inputs produced by MIMICRY. In fact, the non-preservation of the target class generally enhances both validity and label preservation, especially with D_c pairs, highlighting the importance of these factors in evaluating DL effectiveness.

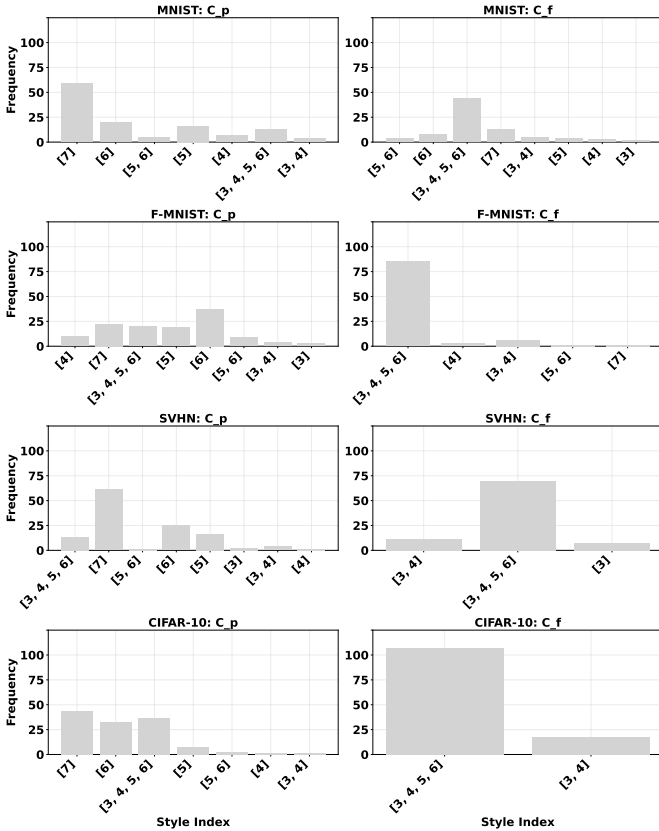


Fig. 6. RQ4: Layers usage for StyleMix.

RQ2: *The boundary inputs by MIMICRY exhibit a high validity rate ($\approx 81\%$) and label preservation rate ($\approx 65\%$), according to human assessors.*

3) *RQ3 (Performance):* Figure 5 presents boxplots illustrating the number of iterations required to identify boundary inputs. For the sake of space, we discuss only two configurations for each dataset: partial-confidence seeds and full-confidence seeds that achieve target preservation. Other configurations exhibit similar distributions. Our results indicate that partial-confidence configurations consistently identify boundary inputs more quickly than full-confidence configurations. This outcome is expected because full-confidence seeds are typically distant from the boundary, requiring MIMICRY to use the entire budget for identifying the boundary.

RQ3: *MIMICRY is notably faster at exposing boundary inputs for partial-confidence seeds compared to full-confidence seeds, with performance improvements ranging from $5\times$ on CIFAR-10 to $19\times$ on MNIST.*

4) *RQ4 (Configuration):* Figure 6 illustrates the frequency of layers used for style mixing among the seeds for which the boundary is successfully found. The results are presented for each dataset separately. For clarity, we include only two

configurations for each dataset: partial-confidence seeds and full-confidence seeds. Other configurations are omitted as they exhibit similar distributions. For partial-confidence seeds, there is a broad distribution of layers used for style mixing, with the finest-grained layers (e.g., 6 and 7) frequently chosen to minimize changes. In contrast, for full-confidence seeds, MIMICRY employs a combination of layers [3, 4, 5, 6], indicating that a mix of both fine and middle layers is required to achieve boundary inputs.

RQ4: *MIMICRY mostly employs the finest-grained layers to generate boundary inputs for partial-confidence seeds. In contrast, full-confidence seeds require a combination of both fine and middle layers to generate boundary inputs.*

5) *RQ5 (Comparison):* We use the best configurations found in the previous research questions, i.e., MIMICRY without target preservation, to perform a comparison with DeepJanus. Table II presents, for all datasets, the results of the comparison. The table shows, for each tool, the number of boundary inputs, the label coverage, as well as the validity and label preservation results from the human study. Overall, MIMICRY generated more boundary inputs than DeepJanus (+157% for MNIST, +100% for FashionMNIST, and +452% for SVHN). These inputs contribute to covering a larger boundary with other classes, as indicated by the label coverage (+30% for MNIST, +3% for FashionMNIST, and +248% for SVHN). More details about the label coverage among the different configurations of MIMICRY are available in Figure 7. It is notable that for the CIFAR-10, the label coverage rate for each source class is very high (over 90%). However, the label coverage for MIMICRY with C_f and target preservation performs poorly due to a lack of samples. Concerning validity and label preservation, both techniques score good results, with the main difference being for FashionMNIST, where MIMICRY achieves a validity rate 37% higher.

RQ5: *MIMICRY generates more boundary inputs than DeepJanus. These boundary inputs are characterized by higher quality in terms of validity, label preservation rate, and label coverage across all datasets.*

H. Threats to Validity

1) *Internal validity:* We conducted comparisons between all variants of MIMICRY and the baseline using the same experimental framework and pool of seeds. Additionally, regarding the StyleGAN models, we utilized pre-trained models available from the literature [24]. When not available, we trained the StyleGAN models using the scripts available in the replication package of the original paper [24], as it is difficult to envision less threat-prone approaches. Our manual analysis of the seeds also represents a potential threat to validity. Our human evaluation of the outputs generated using these seeds also implicitly confirms the reliability of the initial seeds.

TABLE II
RQ₅: COMPARISON OF MIMICRY WITH DEEPJANUS.

	MIMICRY				DeepJanus			
	Boundary Inputs	Label Coverage	Validity	Label Preservation	Boundary Inputs	Label Coverage	Validity	Label Preservation
MNIST	162	0.64	0.98	0.95	63	0.49	0.94	0.91
FashionMNIST	176	0.74	0.78	0.69	88	0.72	0.57	0.41
SVHN	171	0.80	0.94	0.70	31	0.23	0.87	0.64

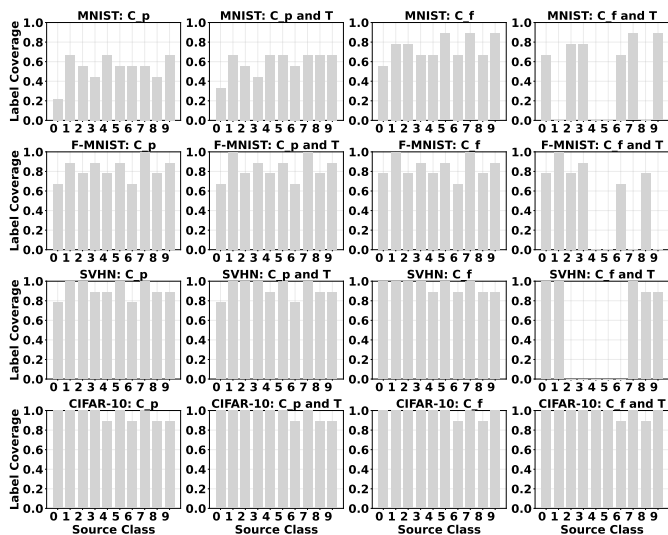


Fig. 7. RQ₅: Label Coverage.

2) *External validity*: The limited number of DL systems included in our evaluation poses a threat to the generalizability of our results. We addressed this issue by incorporating a variety of datasets with increasing complexity and high-performing models from related literature. We demonstrated the usefulness of the original StyleGAN architecture [24]; however, other style-based architectures [29], [37], [40] may also yield promising results.

V. DISCUSSION

A. Style-Based GANs for Boundary Testing

Our experiments showed the effectiveness of style-based GANs for boundary testing of DL systems. These networks are typically used to generate ultra-realistic images thanks to their high degree of control of both low-level and high-level image characteristics. In this paper, we show how to leverage this property for testing, specifically for boundary analysis of DL systems, an important yet challenging open problem in the literature.

Our approach depends on the quality of the style-based GANs, i.e., on their capability to constitute a correct reference of the DL system’s data distribution, once trained. Well-trained GANs better capture the relevant structures in a distribution, thus producing image seeds that are of high quality (i.e., valid in-distribution inputs for the DL system under test). In

contrast, GANs with poor training or bugs might produce invalid inputs. In our study, we trained robust GANs that demonstrated a high source seed validity rate upon manual inspection. Additionally, we conducted a human evaluation of the outputs generated using these seeds. The high validity rate of these outputs implicitly validates the initial seeds, due to the minimal targeted modifications introduced by our approach.

Our findings highlight the substantial advantages of using style-based GANs for boundary testing. These GANs facilitate low-level modifications of the DNN’s input seeds while maintaining the validity and relevance of the tests to the original input domain. A key benefit of MIMICRY is its model- and system-agnostic nature. It requires only a black-box access to the training dataset, without necessitating any modifications to the DL system being tested.

B. MIMICRY’s Configurations

All configurations of MIMICRY demonstrate consistent effectiveness across all iterations. However, our findings indicate that selecting the optimal style vector depends on specific seeds and their associated DL system’s confidence. We evaluated four distinct image classifiers from various domains (e.g., digits, clothes). MIMICRY maintained its effectiveness across different datasets and configurations. We attribute this to its direct manipulation of the image’s style within the latent space, which also positively impacts boundary testing. Quite importantly, MIMICRY generates boundary inputs while retaining the essential properties of validity and label preservation, ensuring that the tests fulfill their intended purpose.

The comparison with DeepJanus has produced positive results for MIMICRY, demonstrating competitive performance across all metrics. One significant aspect is the balance between exploration and exploitation. DeepJanus is designed to prioritize exploration within its fitness function, whereas MIMICRY adopts a more targeted approach by requiring a target seed. Despite this difference, our results show that MIMICRY achieves superior label coverage, contributing to both the exploration and exploitation of the label space of failures. This is due to the explicit control that MIMICRY has over the target boundary, in contrast to DeepJanus.

VI. RELATED WORK

The three main families of DL test generation are model-based input representation, raw input manipulation, and latent space manipulation. We overview the main propositions next.

A. Model-based Input Manipulation

Model Input Manipulation (MIM) techniques leverage a model of the input domain to generate test inputs, similar to conventional model-driven engineering practices that uphold compliance with domain-specific constraints [5], [20], [41]–[44]. The manipulation occurs on the model, which is subsequently reconverted to the original format [45].

MIM techniques operate within a restricted input space, specifically the control parameters of the model representation. These techniques enhance the realism of the produced outputs by implementing appropriate model constraints.

Several search-based MIM approaches have been applied to DL-based image classifiers. DeepHyperion [28] uses the MAP-Elites Illumination Search algorithm [46] to explore the feature space of the input domain and identify misbehavior-inducing features. DeepMetis [47] a MIM approach that generates inputs that behave correctly on original DL models and misbehave on mutants obtained through injection of realistic faults [4], which can be useful to enhance the mutation killing ability of a test set.

DeepJanus [5] is the MIM approach most related to this work since it performs boundary testing of DL systems. Therefore, we performed an explicit empirical comparison with the DeepJanus approach in this work.

However, a significant limitation of MIM approaches is their reliance on the availability of a high-quality model representation for the specific input domain, which is manually crafted [48]. Unlike MIM techniques, MIMICRY leverages a generative network to learn the distribution of the input domain. This approach is largely automated and requires no labeling or other cost, except for hyperparameter tuning. This characteristics of MIMICRY broadens its applicability across various domains.

B. Raw Input Manipulation

Raw input manipulation (RIM) techniques involve modifying an image’s original pixel space to create a new input by perturbing the pixel values.

DeepXplore [8] employs various techniques, including occlusion, light manipulation, and blackout to cause misbehaviors. These perturbations are intended to improve neuron coverage within the DL system. DLFuzz [49] introduces noise to the seed image to increase the likelihood of system misbehavior. DLFuzz generates adversarial inputs for DL systems without relying on cross-referencing other similar DL systems or manual labeling. DeepTest [7] alters the images using synthetic affine transformation from the computer vision domain, such as blurring and brightness adjustments, to create simulated rain/fog effects.

RIM techniques aim to produce minimal, often imperceptible changes to original to trigger misbehaviors in the DL system. However, since RIM techniques are limited to modifying existing inputs, they cannot thoroughly explore the input domain and its boundaries, while generative DL models can sample novel inputs from the data distribution. Moreover,

the manipulated images might not always represent real-world functional inputs, e.g., images with artificial artifacts at the corners or unnatural lighting conditions generated by DeepXplore. Consequently, such techniques are more suitable for security and robustness testing rather than for functional testing [48].

Differently, our technique targets functional testing, specifically boundary value analysis of DL systems. We achieve this by using style-mixing operations in the latent space to generate inputs beyond the original datasets, while remaining within the same distribution.

C. Latent Space Manipulation

Latent space manipulation techniques generate new inputs by learning and reconstructing the underlying distribution of the input data. The most commonly used techniques are Variational Autoencoders (VAE) [50], [51] and Generative Adversarial Networks (GAN) [21], [22].

Sinvad [13] constructs the input space using VAE and navigates the latent space by adding a random value sampled from a normal distribution to a single element of the latent vector. Sinvad aims to explore the latent space by maximizing either the probability of misbehaviors, estimated from the softmax layer output, or by surprise coverage [11].

The Feature Perturbations technique [15], [16] involves injecting perturbations into the output of the generative model’s first layers, which represent high-level features of images. These perturbations can affect various characteristics of the image, such as shape, location, texture, or color. DeepRoad [6] generates driving images using Generative Adversarial Networks (GANs) for image-to-image translation.

CIT4DNN [14] combines VAE and combinatorial testing [52]. This allows the systematic exploration and generation of diverse and infrequent input datasets. CIT4DNN partitions latent spaces to create test sets that contain a wide range of feature combinations and rare occurrences. A recently proposed technique, Instance Space Analysis, aims to pinpoint the critical features of test scenarios that impact the detection of unsafe behavior [20].

Differently from such latent space manipulation techniques, we leverage the style-mixing operations in the latent space for boundary value analysis of DL systems to characterize the frontier of behaviors instead of simply revealing misbehaviors. Our style-mix latent operations for functional testing represent a new contribution to the state of the art.

VII. CONCLUSIONS AND FUTURE WORK

In this paper, we present and evaluate MIMICRY, a testing tool designed for deep learning (DL) systems. MIMICRY generates boundary inputs through mutations derived from style-based generative adversarial networks. The core concept of MIMICRY lies in the systematic modification of the latent code of a generated class element within the latent space, enabling precise assessment of the modifications’ impacts in the image space.

We conducted evaluations of MIMICRY on DL image classifiers. Our empirical studies demonstrate that MIMICRY is highly effective at generating boundary inputs for seeds, regardless of their proximity to the boundary. It achieves this quickly while maintaining high validity and label preservation rates. Furthermore, our results indicate that MIMICRY significantly outperforms a baseline model-level approach in terms of effectiveness, while also preserving a high validity rate for failing test inputs.

Future work will involve extending the comparison to additional benchmarks and exploring the applicability of StyleGAN inversion techniques, such as Pivotal Tuning for Latent-based Editing of Real Images (PTI). This will enable us to invert labeled data from the test dataset back into latent space representations.

REFERENCES

- [1] H. Schütze, C. D. Manning, and P. Raghavan, *Introduction to information retrieval*. Cambridge University Press Cambridge, 2008, vol. 39.
- [2] V. Riccio, G. Jahangirova, A. Stocco, N. Humbatova, M. Weiss, and P. Tonella, “Testing machine learning based systems: a systematic mapping,” *Empirical Software Engineering*, vol. 25, pp. 5193–5254, 2020.
- [3] J. M. Zhang, M. Harman, L. Ma, and Y. Liu, “Machine learning testing: Survey, landscapes and horizons,” *IEEE Transactions on Software Engineering*, vol. 48, no. 1, pp. 1–36, 2020.
- [4] N. Humbatova, G. Jahangirova, G. Bavota, V. Riccio, A. Stocco, and P. Tonella, “Taxonomy of real faults in deep learning systems,” in *Proceedings of 42nd International Conference on Software Engineering*, ser. ICSE ’20. New York, NY, USA: ACM, 2020, p. 12 pages.
- [5] V. Riccio and P. Tonella, “Model-based exploration of the frontier of behaviours for deep learning system testing,” in *Proceedings of the 28th ACM Joint Meeting on European Software Engineering Conference and Symposium on the Foundations of Software Engineering*, ser. ESEC/FSE ’20, 2020, pp. 876–888.
- [6] M. Zhang, Y. Zhang, L. Zhang, C. Liu, and S. Khurshid, “Deeproad: Gan-based metamorphic testing and input validation framework for autonomous driving systems,” in *Proceedings of the 33rd ACM/IEEE International Conference on Automated Software Engineering*, ser. ASE 2018. New York, NY, USA: ACM, 2018, pp. 132–142. [Online]. Available: <http://doi.acm.org/10.1145/3238147.3238187>
- [7] Y. Tian, K. Pei, S. Jana, and B. Ray, “Deepest: Automated testing of deep-neural-network-driven autonomous cars,” in *Proceedings of the 40th International Conference on Software Engineering*, ser. ICSE ’18. New York, NY, USA: ACM, 2018, pp. 303–314. [Online]. Available: <http://doi.acm.org/10.1145/3180155.3180220>
- [8] K. Pei, Y. Cao, J. Yang, and S. Jana, “Deepxplore: Automated whitebox testing of deep learning systems,” in *Proceedings of the 26th Symposium on Operating Systems Principles*, ser. SOSP ’17, vol. 62, no. 11. New York, NY, USA: ACM, oct 2017, pp. 1–18. [Online]. Available: <http://doi.acm.org/10.1145/3132747.3132785>
- [9] Y. Sun, X. Huang, D. Kroening, J. Sharp, M. Hill, and R. Ashmore, “Testing deep neural networks,” *arXiv preprint arXiv:1803.04792*, 2018.
- [10] L. Ma, F. Juefei-Xu, F. Zhang, J. Sun, M. Xue, B. Li, C. Chen, T. Su, L. Li, Y. Liu *et al.*, “Deepgauge: Multi-granularity testing criteria for deep learning systems,” in *Proceedings of the 33rd ACM/IEEE international conference on automated software engineering*, ser. ASE 2018. New York, NY, USA: ACM, 2018, pp. 120–131. [Online]. Available: <http://doi.acm.org/10.1145/3238147.3238202>
- [11] J. Kim, R. Feldt, and S. Yoo, “Guiding deep learning system testing using surprise adequacy,” in *2019 IEEE/ACM 41st International Conference on Software Engineering (ICSE)*, ser. ICSE ’19, IEEE, Piscataway, NJ, USA: IEEE Press, 2019, pp. 1039–1049. [Online]. Available: <https://doi.org/10.1109/ICSE.2019.00108>
- [12] Y. Liu, L. Feng, X. Wang, and S. Zhang, “Deepboundary: A coverage testing method of deep learning software based on decision boundary representation,” in *2022 IEEE 22nd International Conference on Software Quality, Reliability, and Security Companion (QRS-C)*. IEEE, 2022, pp. 166–172.
- [13] S. Kang, R. Feldt, and S. Yoo, “Sinvad: Search-based image space navigation for dnn image classifier test input generation,” in *Proceedings of the IEEE/ACM 42nd International Conference on Software Engineering Workshops*, 2020, pp. 521–528.
- [14] S. Dola, R. McDaniel, M. B. Dwyer, and M. L. Soffa, “Cit4dnn: Generating diverse and rare inputs for neural networks using latent space combinatorial testing,” in *Proceedings of the IEEE/ACM 46th International Conference on Software Engineering*, 2024, pp. 1–13.
- [15] I. Dunn, T. Melham, and D. Kroening, “Semantic adversarial perturbations using learnt representations,” *CoRR*, vol. abs/2001.11055, 2020. [Online]. Available: <https://arxiv.org/abs/2001.11055>
- [16] I. Dunn, H. Pouget, D. Kroening, and T. Melham, “Exposing previously undetectable faults in deep neural networks,” in *Proceedings of the 30th ACM SIGSOFT International Symposium on Software Testing and Analysis*, 2021, pp. 56–66.
- [17] M. Pezzè and M. Young, *Software testing and analysis: process, principles, and techniques*. John Wiley & Sons, 2008.
- [18] H. Fahmy, F. Pastore, L. Briand, and T. Stifter, “Simulator-based explanation and debugging of hazard-triggering events in dnn-based safety-critical systems,” *ACM Transactions on Software Engineering and Methodology*, vol. 32, no. 4, pp. 1–47, 2023.
- [19] M. Biagiola and P. Tonella, “Boundary state generation for testing and improvement of autonomous driving systems,” 2023.
- [20] N. Neelofar and A. Aleti, “Identifying and explaining safety-critical scenarios for autonomous vehicles via key features,” *ACM Transactions on Software Engineering and Methodology*, vol. 33, no. 4, pp. 1–32, 2024.
- [21] I. Goodfellow, J. Pouget-Abadie, M. Mirza, B. Xu, D. Warde-Farley, S. Ozair, A. Courville, and Y. Bengio, “Generative adversarial nets,” *Advances in neural information processing systems*, vol. 27, pp. 2672–2680, 2014. [Online]. Available: <http://papers.nips.cc/paper/5423-generative-adversarial-nets.pdf>
- [22] —, “Generative adversarial networks,” *Communications of the ACM*, vol. 63, no. 11, pp. 139–144, 2020.
- [23] S. Dola, M. B. Dwyer, and M. L. Soffa, “Input distribution coverage: Measuring feature interaction adequacy in neural network testing,” *ACM Transactions on Software Engineering and Methodology*, vol. 32, no. 3, pp. 1–48, 2023.
- [24] T. Karras, S. Laine, and T. Aila, “A style-based generator architecture for generative adversarial networks,” *CoRR*, vol. abs/1812.04948, 2018. [Online]. Available: <http://arxiv.org/abs/1812.04948>
- [25] X. Huang and S. Belongie, “Arbitrary style transfer in real-time with adaptive instance normalization,” in *Proceedings of the IEEE International Conference on Computer Vision (ICCV)*, 10 2017.
- [26] V. Riccio and P. Tonella, “When and why test generators for deep learning produce invalid inputs: an empirical study,” in *Proceedings of 45th International Conference on Software Engineering*, ser. ICSE ’23. ACM, 2023, p. 12 pages.
- [27] M. Weiss and P. Tonella, “Fail-safe execution of deep learning based systems through uncertainty monitoring,” in *IEEE 14th International Conference on Software Testing, Validation and Verification*, ser. ICST ’21. IEEE, 2021.
- [28] T. Zohdinasab, V. Riccio, A. Gambi, and P. Tonella, “Deephyperion: exploring the feature space of deep learning-based systems through illumination search,” in *Proceedings of the 30th ACM SIGSOFT International Symposium on Software Testing and Analysis*, ser. ISSTA ’21. Association for Computing Machinery, 2021, pp. 79–90.
- [29] T. Karras, M. Aittala, J. Hellsten, S. Laine, J. Lehtinen, and T. Aila, “Training generative adversarial networks with limited data,” *CoRR*, vol. abs/2006.06676, 2020. [Online]. Available: <https://arxiv.org/abs/2006.06676>
- [30] Z. Wang, A. Bovik, H. Sheikh, and E. Simoncelli, “Image quality assessment: from error visibility to structural similarity,” *IEEE Transactions on Image Processing*, vol. 13, no. 4, pp. 600–612, 2004.
- [31] Y. LeCun, L. Bottou, Y. Bengio, and P. Haffner, “Gradient-based learning applied to document recognition,” *Proceedings of the IEEE*, vol. 86, no. 11, pp. 2278–2324, 1998.
- [32] H. Xiao, K. Rasul, and R. Vollgraf, “Fashion-mnist: a novel image dataset for benchmarking machine learning algorithms,” *CoRR*, vol. abs/1708.07747, 2017. [Online]. Available: <http://arxiv.org/abs/1708.07747>
- [33] Y. Netzer, T. Wang, A. Coates, A. Bissacco, B. Wu, A. Y. Ng *et al.*, “Reading digits in natural images with unsupervised feature learning,” in *NIPS workshop on deep learning and unsupervised feature learning*, vol. 2011, no. 2. Granada, 2011, p. 4.

- [34] A. Krizhevsky, "Learning multiple layers of features from tiny images," pp. 32–33, 2009. [Online]. Available: <https://www.cs.toronto.edu/~kriz/learning-features-2009-TR.pdf>
- [35] J. T. Springenberg, A. Dosovitskiy, T. Brox, and M. Riedmiller, "Striving for simplicity: The all convolutional net," *arXiv preprint arXiv:1412.6806*, 2014.
- [36] A. Dosovitskiy, L. Beyer, A. Kolesnikov, D. Weissenborn, X. Zhai, T. Unterthiner, M. Dehghani, M. Minderer, G. Heigold, S. Gelly, J. Uszkoreit, and N. Houlsby, "An image is worth 16x16 words: Transformers for image recognition at scale," 2021. [Online]. Available: <https://arxiv.org/abs/2010.11929>
- [37] T. Karras, S. Laine, M. Aittala, J. Hellsten, J. Lehtinen, and T. Aila, "Analyzing and improving the image quality of stylegan," *CoRR*, vol. abs/1912.04958, 2019. [Online]. Available: <http://arxiv.org/abs/1912.04958>
- [38] M. Heusel, H. Ramsauer, T. Unterthiner, B. Nessler, G. Klambauer, and S. Hochreiter, "Gans trained by a two time-scale update rule converge to a nash equilibrium," *CoRR*, vol. abs/1706.08500, 2017. [Online]. Available: <http://arxiv.org/abs/1706.08500>
- [39] S. J. Stratton, "Population research: Convenience sampling strategies," *Prehospital and Disaster Medicine*, vol. 36, no. 4, p. 373–374, 2021.
- [40] T. Karras, M. Aittala, S. Laine, E. Härkönen, J. Hellsten, J. Lehtinen, and T. Aila, "Alias-free generative adversarial networks," *CoRR*, vol. abs/2106.12423, 2021. [Online]. Available: <https://arxiv.org/abs/2106.12423>
- [41] R. B. Abdessalem, A. Panichella, S. Nejati, L. C. Briand, and T. Stifter, "Testing autonomous cars for feature interaction failures using many-objective search," in *Proceedings of the 33rd ACM/IEEE International Conference on Automated Software Engineering*, ser. ASE 2018. New York, NY, USA: ACM, 2018, pp. 143–154. [Online]. Available: <http://doi.acm.org/10.1145/3238147.3238192>
- [42] R. Ben Abdessalem, S. Nejati, L. C. Briand, and T. Stifter, "Testing advanced driver assistance systems using multi-objective search and neural networks," in *2016 31st IEEE/ACM International Conference on Automated Software Engineering (ASE)*, Sep. 2016, pp. 63–74.
- [43] R. Ben Abdessalem, S. Nejati, L. C. Briand, and T. Stifter, "Testing vision-based control systems using learnable evolutionary algorithms," in *2018 IEEE/ACM 40th International Conference on Software Engineering (ICSE)*, May 2018, pp. 1016–1026.
- [44] A. Gambi, M. Mueller, and G. Fraser, "Automatically testing self-driving cars with search-based procedural content generation," in *Proceedings of the 28th ACM SIGSOFT International Symposium on Software Testing and Analysis*, ser. ISSTA 2019. New York, NY, USA: ACM, 2019, pp. 318–328. [Online]. Available: <http://doi.acm.org/10.1145/3293882.3330566>
- [45] C. Larman *et al.*, *Applying UML and patterns*. Prentice Hall Upper Saddle River, 1998, vol. 2.
- [46] J. Mouret and J. Clune, "Illuminating search spaces by mapping elites," *CoRR*, vol. abs/1504.04909, 2015. [Online]. Available: <http://arxiv.org/abs/1504.04909>
- [47] V. Riccio, N. Humbatova, G. Jahangirova, and P. Tonella, "Deepmetis: Augmenting a deep learning test set to increase its mutation score," in *Proceedings of the 36th IEEE/ACM International Conference on Automated Software Engineering*, ser. ASE '21. IEEE/ACM, 2021.
- [48] V. Riccio and P. Tonella, "When and why test generators for deep learning produce invalid inputs: an empirical study," in *2023 IEEE/ACM 45th International Conference on Software Engineering (ICSE)*, 2023, pp. 1161–1173.
- [49] J. Guo, Y. Jiang, Y. Zhao, Q. Chen, and J. Sun, "Dlfuzz: Differential fuzzing testing of deep learning systems," in *Proceedings of the 2018 26th ACM Joint Meeting on European Software Engineering Conference and Symposium on the Foundations of Software Engineering*, 2018, pp. 739–743.
- [50] D. P. Kingma and M. Welling, "Auto-encoding variational bayes," *arXiv preprint arXiv:1312.6114*, 2013.
- [51] C. Doersch, "Tutorial on variational autoencoders," *arXiv preprint arXiv:1606.05908*, 2016.
- [52] D. Cohen, S. Dalal, M. Fredman, and G. Patton, "The aetg system: an approach to testing based on combinatorial design," *IEEE Transactions on Software Engineering*, vol. 23, no. 7, pp. 437–444, 1997.